Title

Analyzing inflammatory signatures of letrozole-induced mouse model of polycystic ovary syndrome

Permalink

https://escholarship.org/uc/item/9p27d515

Author

De Robles, Gabriela

Publication Date

2023

Peer reviewed|Thesis/dissertation

UNIVERSITY OF CALIFORNIA,
IRVINE

Analyzing inflammatory signatures of letrozole-induced mouse model of polycystic ovary
syndrome

THESIS

submitted in partial satisfaction of the requirements
for the degree of

MASTER OF SCIENCE

in Mathematical, Computational, and Systems Biology

by

Gabriela De Robles

Thesis Committee:
Assistant Professor Dequina Nicholas, Chair
Assistant Professor Marcus Seldin
Professor Charles Glabe

2023

TABLE OF CONTENTS

Page

LIST OF FIGURES

LIST OF TABLES

ACKNOWLEDGEMENTS

I would like to express the deepest appreciation to my committee chair, Dr. Dequina Nicholas, and my labmates for their consistent support and guidance.

ABSTRACT OF THE THESIS

Analyzing inflammatory signatures of letrozole-induced mouse model of polycystic ovary

syndrome

by

Gabriela De Robles

Master of Science in Mathematical, Computational, and Systems Biology

University of California, Irvine, 2023

Assistant Professor Dequina Nicholas, Chair

Polycystic ovary syndrome (PCOS), is the most common endocrine disorder affecting both the reproduction and metabolism of females. Characteristics of this heterogeneous disorder include anovulation, biochemical hyperandrogenemia, insulin resistance, and obesity, which can be recapitulated with a letrozole-induced PCOS mouse model. Immune abnormalities have also been reported in PCOS human patients, including pro-inflammatory factor secretion imbalance and endothelial cell dysfunction. The extent to which the letrozole-induced mouse model for PCOS can represent these immune dysregulations remain unclear, specifically its relevance to disrupting hormone-regulating centers, such as the pituitary gland. Using a PCOS mouse model developed via letrozole induction, we performed single-cell mRNA sequencing (scRNA-seq) on the pituitaries to study impairment in hormone activity and immune regulation. A multiplexed immunoassay was also carried out on stimulated splenocytes to profile cytokines under different immune cell stimulation conditions. The scRNA-seq on the pituitaries revealed microglia and B cells, including sub-populations of macrophages, neutrophils, and T memory cells. Gene set

enrichment analysis revealed an association of differentially expressed genes, including *Prl*, in the total immune cell population of PCOS mice with inflammatory response and positive regulation of cytokine production. Pituitary neuroendocrine cell types also exhibited dysregulated expression, including lactotropes, corticotropes, somatotropes, and two separate clusters of gonadotropes. Interestingly, the lactotrope population decreased in PCOS mice, which could indicate an effect on the total prolactin secretion. Differences in cytokine expression from the multiplex immunoassays also allowed the distinction of mice treated with or without letrozole via partial least square discriminate analysis. Altogether, the letrozole-treated mice presented disrupted immune responses and hormonal imbalances in their transcription and cytokine profiles that provided additional insight to their ability to model the PCOS immune system.

INTRODUCTION

With a worldwide prevalence of 4-20% among reproductive-aged women, polycystic ovary syndrome (PCOS) is the most common endocrine disorder affecting reproductive, metabolic, and cardiovascular health (1). Treatments are available to manage PCOS symptoms; however, poor understanding of the pathophysiological mechanisms has hindered the development of a cure (2). Various animal models of PCOS have been utilized to identify specific underlying causes of the disorder, such as the aromatase-inhibitor model (3). Prepubertal female mice treated with letrozole, one such aromatase inhibitor, generate PCOS-like traits via endogenous hyperandrogenemia, resulting in acyclicity, polyfollicular ovaries, increased body weight, and insulin resistance (4). Variable reproductive and metabolic phenotypes are produced depending on the animal model and induction method chosen, but the letrozole-treated PCOS mouse model is frequently used and well established in studying the pathophysiology under excess androgen.

In addition to the established phenotypes defining PCOS, evidence of persistent low-grade inflammation in patients is increasing (5-7). Elevated inflammatory cytokine levels in the plasma of PCOS patients have been reported, while increased cytokine expression observed in the endometrium has been proposed to be a result of hyperandrogenism (8-12). Alterations in local cytokine production have also varied across different tissues. In a comparison between PCOS and non-PCOS ovaries, Th1 cytokine production was significantly higher in PCOS ovaries, while the production of Th2 cytokines displayed no significant difference between the two groups (13). The extent to which animal models reflect this low-grade inflammation in PCOS is under investigation, to determine whether it could be utilized to further understand the role of immune dysfunctions in the pathophysiology of PCOS.

1

While the reproductive organs of PCOS patients have been a main research focus in studying immune dysregulation, the upstream tissues of the hypothalamic-pituitary-gonadal (HPG) axis are another important component to consider (14,15). Defects in the HPG axis can result in hyperandrogenism, where hypothalamic inflammation has been proposed as a possible contributor to the pathogenesis of PCOS (16-18). Besides the hypothalamus, the anterior pituitary is another regulatory center linked to hormonal imbalances reported in PCOS patients (19). Secretion of gonadotropin-releasing hormone (GnRH) from the hypothalamus regulates the release of luteinizing hormone (LH); however, increased GnRH pulses in PCOS animal models have resulted in various LH level changes (20-22). Furthermore, the inflammatory state of the pituitary in PCOS animal models remains insufficiently examined in comparison to the hypothalamus. In this study, we performed scRNA-seq on the anterior pituitaries of letrozole-induced prepubertal female mice and analyzed cytokine expression profiles from stimulated splenocytes to investigate the potential links among hormone activity, immune regulation, and inflammation in PCOS patients.

MATERIALS & METHODS

PCOS mouse model

Four-week-old C57BL/6 female mice (Jackson) were housed under specific pathogen-free conditions in a vivarium with ad libitum access to standard chow and water. An automatic 12h:12h light/dark cycle (light period: 06.00-18.00) was set in the vivarium. All animal procedures proceeding with this study were approved by the University of California, Irvine AUP-21-059. Before the treatment, the mice were weighed and sorted to establish similar starting weights in both treatment groups. The PCOS mouse model was induced via subcutaneous implantation of a 3 mg 60-day slow-release letrozole (LET) or

2

placebo pellet (3 mm diameter; Innovative Research of America). For five weeks, the mice underwent the treatment where the letrozole pellet was expected to release the aromatase inhibitor at a slow, constant rate (50 µg/day). The two mice groups, LET and control, were housed in separate cages with either 4 or 5 mice in each to avoid any influence of coprophagy. At the end of the 5-week treatment, the mice were euthanized using CO_2 followed by cervical dislocation and decapitation. This procedure was done in two cohorts of mice and resulted in n=9 mice per group, LET and control.

Reproductive and metabolic phenotype analysis

The mice were weighed weekly. On week 4 of the treatment, the mice underwent a glucose tolerance test (GTT) following a 6 hr fast. A handheld blood glucose monitoring system (Contour NEXT ONE, Ascensia Diabetes Care US, Inc.) was used to measure tail blood glucose (Time 0) before an i.p. injection of glucose (1.5g/kg) body weight in sterile phosphate-buffered saline). At 15, 30, 60, 90 and 120 minutes post injection, tail blood glucose was again measured. On week 5 of the treatment, vaginal epithelium smears of the mice were collected daily for seven days. The stage of the estrous cycle was determined for each day based on the predominant cell type in the smears.

Pituitary gland dissociation and immune cell enrichment

The pituitary glands were dissected out of the mice at the end of the 5-week treatment and dispersed by incubation with 0.25% collagenase Type IV and 0.25% trypsin–EDTA (1x) (Life Technologies) as published previously. Pituitaries from control and LET mice were pooled and underwent immune cell enrichment. Using MACS magnetic column separation, the cells were enriched via a CD45+ selection according to the protocol. Both the CD45+ immune cells and CD45-depleted pituitaries were collected for sequencing.

Single-cell mRNA library preparation and sequencing

scRNA-seq libraries were prepared using the 10X Genomics Chromium Single Cell 3'

Reagent Kit v3.1 and 10X Genomics Chromium Single Cell 5' Reagent Kit v2 (10x Genomics,

Pleasanton, CA) according to the manufacturer's protocol. At a capture target set to 10,000

cells, the resulting cDNA from reverse transcription in Gel-in-Emulsion (GEMs) was cleaned

using Dynabeads MyOne SILANE (Life Technologies, Carlsbad, CA) before an 11-cycle

amplification. This amplification occurred with sc5' feature cDNA primers for the

construction of the 5' gene expression libraries. The amplified cDNA was purified with 0.6X

SPRIselect beads (Beckman Coulter, Indianapolis, IN) and underwent quality control using

the Qubit DNA HS assay (Life Technologies, Carlsbad, CA) and the Agilent 2100 Bioanalyzer

DNA HS (Agilent, Santa Clara, CA). PCR amplifications with primers to both the T and B cells

were used to enrich full-length V(D)J segments for the 5' gene expression libraries. Library

construction was done following the 10x workflow with the cDNA fraction. The previous

two quality control assays were used on the constructed libraries before being quantified

by the Kapa qPCR library (Roche, Basel, Switzerland). The libraries were sequenced using

the Illumina NovaSeq 6000 (Illumina, San Diego, CA), in which the cycle numbers were set

to 28 for read 1, 8 for the index read, and 100 for read 2.

Cell ranger, Loupe genome browser, cell type identification

The paired-end sequencing reads were uploaded to the 10x Genomics Cloud

analysis to prep the data for downstream analysis. The Cell Ranger count pipeline (v7.0.1)

was applied to perform a read alignment to the Mus musculus genome (mm10) and build a

feature-barcode matrix of transcriptomes from individual cells. Reads mapping to intronic

regions were included. The Cell Ranger aggr pipeline (v7.0.1) was applied to the outputs

from the count pipeline to normalize the average read depths per cell before merging the datasets. The output from the aggr pipeline was loaded to Loupe Browser (6.1.0) for further downstream analysis.

A quality check was performed to filter out cells with low sequencing complexity. Cells containing a high percentage (>0.05) of UMIs associated with mitochondrial genes were discarded. Additional cells were removed if their UMI count fell outside the threshold, 300 to 20,000 counts, and the number of detected genes was fewer than 100 or exceeded 4,000. These filters resulted in 21,976 cells that underwent Louvain clustering in Loupe.

Identification of the cell types in each cluster was determined based on their top up-regulated genes input into the PanglaoDB database (23) and the expression of anterior pituitary endocrine markers. Cell clusters identified as either non-pituitary endocrine or non-immune (i.e., neurons, fibroblasts, endothelial cells, red blood cells, and stem cells) and those undergoing apoptosis were removed for further downstream analysis. The remaining reclustered cells resulted in 6,966 total cells from the control mice and 4,597 total cells from the LET mice.

Differential expression analysis and enrichment analysis

Besides determining cell clusters, differential expression analysis (DEA) was performed in the Loupe browser between control and LET mice on individual cell clusters. Differentially expressed genes (DEGs) with a |Log2FC|≥1.5 and p-value≤0.05 were accepted for further analysis. To determine the molecular functions and biological pathways associated with a list of DEGs in a cluster, GO enrichment analysis (GEA) was performed using the web-based PANTHER 17.0 tool (24,25,26). For the lactotrope population, a gene set enrichment analysis (GSEA) was performed using R (4.2.3).

Splenocyte stimulation and cytokine multiplex immunoassay

At the end of the 5-week treatment, the spleen of the mice were collected. The spleen cells were mechanically dissociated and stimulated (200,000 cells/200 mL) with either mouse T-activator CD3/CD28 dynabeads (1 bead per cell; ThermoFisher) or lipopolysaccharide O111:B4 (conc.; Ebioscience) for 40 hours at 37 °C. The conditioned media from the stimulated splenocyte cells for each mouse were collected and stored at -20°C. A total of 30 cytokines and chemokines were quantified using the Milliplex MAP mouse Th17 magnetic bead panel and the Milliplex MAP mouse cytokine/chemokine magnetic bead panel (Millipore Sigma) according to the protocol from each respective kit. The analyte concentrations were measured using an Intelliflex instrument (Luminex) and the Belysa software (1.2). Two, separate datasets of cytokine quantifications were generated based on whether the supernatant originated from splenocytes activated with either CD3/28 dynabeads or LPS.

Normalization, batch effect correction

Computational analysis of the two cytokine datasets was conducted in R (4.2.3) individually. The measurements underwent a z-score normalization and were evaluated for the presence of batch effects. The predicted batch effect between the two mice cohorts was corrected using the Combat function in the SVA package. In Graphpad (9.5.1), 5.46% of outliers were detected in the total analyte measurements and removed before being replaced based on iterative, principal component analysis (PCA) modeling.

Partial least squares modeling

Partial least squares discriminate analysis (PLS-DA) was done for the two datasets of cytokine quantifications separately using Solo (Eigenvector Research, Inc.). The cytokine

measurements were assigned as the independent variable, while the discrete regression variable was the treatment classification, LET or control. Two primary latent variables, LV1 and LV2, were used in in leave-one-out cross-validation.

Statistical analysis

All the statistical tests were performed across R (4.2.3), Graphpad (9.5.1), Loupe (6.1.0) and PANTHER (24,25,26). In comparisons between the LET and control mice groups, Student t-tests were performed. To compare population percentages, z-tests were performed. All statistical analysis results with a p-value≤0.05 were determined as significant.

RESULTS

Letrozole treatment on prepubertal female mice replicated both metabolic and reproductive characteristics representative of PCOS

To induce PCOS characteristics in a mouse model, prepubertal female mice were implanted with a placebo or LET pellet for 5 weeks (Fig. 1A). A significant difference in body weight was detected by two weeks post-implant, with LET mice having increased weight gain in comparison to control mice (Fig. 1A). After 3 weeks of LET treatment, a glucose tolerance test was performed which revealed significantly higher blood glucose levels in LET mice compared to control mice, indicating impaired glucose absorption by tissues (Fig. 1B). Next, to confirm LET induced reproductive characteristics of PCOS, we examined the estrous cycle during the final week of the letrozole treatment. LET mice spent a significantly longer time in diestrus compared to the control mice (Fig. 1C). While all the control mice went through all stages of the estrous cycle, most of the LET mice remained in only diestrus (Fig. 1D). From these data, namely the high body weight, impaired glucose

7

tolerance, and acyclicity experienced in the LET mice, we conclude that this model, same as published results, recapitulates both reproductive and metabolic phenotypes found in PCOS human patients.

Single-cell mRNA sequencing revealed impaired hormone activity in pituitary endocrine cell populations of letrozole-treated mice

To identify the potential roles of pituitary endocrine cell populations in the phenotypes of PCOS, the pituitary glands of 10 individual C57BL/6 female mice underwent scRNA-seq after a 5-week letrozole treatment. The read depths were normalized and the datasets from both the LET mice and control mice were aggregated together. After filtering out cells with low sequencing complexity and excluding those to be identified as non-pituitary (See Methods and Materials), 4,536 neuroendocrine cells from the control mice and 1,781 neuroendocrine cells from the LET mice remained for downstream analysis. Based on established gene markers for pituitary endocrine cells, populations of somatotropes, lactotropes, corticotropes, melanotropes, and gonadotropes were identified (Fig. 2A and 2B). Interestingly, two different clusters of gonadotropes were generated in the tSNE plot (Fig. 2A and 2B). Thyrotropes are another cell type in the anterior pituitary, but a cluster was not detected likely because it is the least abundant in the organ. Despite the control mice having a higher total number of pituitary endocrine cells, significant population changes occurred (Fig. 2C). Both clusters of gonadotropes and the single cluster of corticotropes had higher population percentages in the LET mice compared to the control mice (p-value: 6.67×10^{-12}, 2.12×10^{-3}, 6.73×10^{-13} respectively). The lactotrope population decreased in the LET mice (p-value: 1.96×10^{-21}), but a denser population of lactotropes in the upper left corner of the cluster concurrently displayed higher expression

of both *Wfdc2* and *Gng3* (Fig. 2A). These two genes are associated with malignant ovarian cyst and breast cancer, respectively, and are included in the list of significant differentially expressed genes (DEGs) between the total lactotropes in LET vs control mice (27,28).

To further understand transcriptional changes regulating hormone production in PCOS, a differential expression analysis (DEA) was performed for each pituitary endocrine cell cluster between the LET and control mice. *Srxn1* was significantly down-regulated (Log2 FC: -1.9) in the corticotropes, while *Crhbp*, the gene expressing corticotropin releasing hormone binding protein, was significantly down-regulated (Log2 FC: -3.12) in the total lactotropes of LET mice. 19 up-regulated genes with a minimum Log2 FC of 1.5 were detected in the total lactotropes of LET mice. These genesa are involved in pathways associated with kinase activity regulation as detected in a gene set enrichment analysis (GSEA) (Fig. 2C). Up-regulated genes in LET mice were also associated with ribosomal protein (Fig. 2C). DEA on the two identified gonadotrope clusters between the LET and control mice was performed separately, which resulted in their own lists of DEGs. While the second gonadotropes cluster did not have *Lhb* as a significant DEG, the first gonadotropes cluster listed *Lhb* as significantly down-regulated (Log2 FC: -2.06) in the LET mice. Plasma luteinizing hormone is known to be higher in PCOS patients, while its transcript levels vary in the PCOS mouse model. The difference in *Lhb* expression between the two gonadotrope clusters could explain this variation reported (3). Furthermore, the gonadotropes 2 cluster had three, significant up-regulated genes known to code for serine proteases in the kallikrein subfamily (Log2 FC: 5.09-3.71). Overall, the scRNA-seq revealed DEGs within the pituitary cell types that indicated substantial remodeling of the pituitary

microenvironment and hormone secreting cells of LET mice compared to control mice. Overall, these data implicate the loss of lactotropes in the etiology of PCOS.

Single-cell mRNA sequencing revealed altered immune profiles in the pituitaries of letrozole-treated mice

The immune cell populations from the scRNA-seq of the pituitaries of the LET and control mice were also analyzed to identify possible immune changes regulating the HPG axis. In total, 2,430 immune cells from the control mice and 2,816 immune cells from the LET mice were identified after filtering out poor-quality cells and reclustering (See Methods and Materials). By analyzing the top up-regulated genes in the 11 clusters formed in the immune cell population, the cells were identified as macrophages, microglia, neutrophils, T memory cells, and B cells (Fig. 3A). Several of these immune cell subgroups including macrophages, neutrophils, and T memory cells, had multiple clusters. Despite the difference in immune cell count, the total macrophages and T memory cells had a higher prevalence in the control mice (p-value: 3.70×10^{-27}, 9.66×10^{-3} respectively) while the LET mice had a higher total neutrophil population (p-value: 1.80 (p-value: 1.80×10^{-63}) (Fig. 3B).

When DEA was performed for each immune cell cluster between LET and control mice, DEGs were detected in the T memory cells, macrophages, and neutrophils. Unexpectedly, *Prl*, the gene that encodes prolactin, was significantly down-regulated (Log2 FC: -3.42) in the macrophages 1 cluster of LET mice. Although *Prl* is a gene marker for lactotropes, its expression has been reported in immune cells where the protein can function similarly as a cytokine (29). *Irf7* was also identified as a significant up-regulated DEG (Log2FC: 1.74) in the macrophage 4 cluster of LET mice. In the T memory cells 1

10

cluster, *Isg15* was significantly up-regulated (Log2FC: 2.89) while the neutrophils 2 cluster had *Lmo4* and *Malat1* as significantly down-regulated (Log2FC: -2.00, -1.67 respectively) in LET mice. For the total neutrophil population with both clusters, 10 significant genes with a minimum Log2 FC of -1.5 were identified in LET mice and inputted for GEA. These down-regulated genes were associated with phospholipase activity and cellular homeostasis (Fig. 3C). 14 significant DEGs were identified for the entire immune population in LET mice with a minimum |Log2 FC| of 1.5, which resulted with GO biological pathway terms such as inflammatory response, positive regulation of cytokine production and granulocyte chemotaxis (Fig. 3D). Altogether, the scRNA-seq revealed immune cell infiltration and cytokine secretion within the pituitary as possible critical factors for HPG axis homeostasis and PCOS.

Multivariate analysis of cytokines distinguished letrozole-treated mice from control

The scRNA-seq of the immune cells in the pituitaries indicated cytokine and chemokine regulation after letrozole treatment, but whether these changes in local pituitary immune cells were reflected at a systemic level was unclear. To gain a better understanding of systemic immune changes in the LET mouse, 40 cytokines were quantified in a multiplexed immunoassay (Milliplex) from the conditioned media of activated splenocytes. The cytokines and chemokine measurements were normalized and corrected for batch effects before performing PCA. 5.46% of the total measurements were identified as outliers, which were removed and replaced based on iterative PCA modeling. T cell specific activation with CD3/CD28 dynabeads resulted in analyte measurements that allowed for LET and control mice to cluster with little overlap in the PCA plot (Fig. 4A). Hierarchal clustering presented similar separation between the two mice groups, with IL-

11

1A, IP-10, MIG, and VEGF being significantly down-regulated in the LET mice (Fig. 4B). The LET and control mice could also be distinguished based on their lipopolysaccharide (LPS) induced cytokine secretion, but not as clearly as that from T cell stimulation (Fig. 5A and 5B). Furthermore, the measurements of IL-4, IL-6, IP-10, MIP1A, and MIG were significantly down-regulated in the LET mice.

The pattern of cytokine secretion was complex and varied between the two mice groups under different immune cell stimulations. Therefore, partial least square discriminate analysis (PLS-DA) was used to build a classification model that could identify cytokines important for the PCOS phenotypes. Reducing the total measurements in a PLS-DA can produce a model to recognize a PCOS-like profile, which may not replicate the significant differences per individual cytokine. The cytokine measurements under T cell activation were reduced to a set of latent variables (LV1 and LV2), where LV1 became a distinguishable variable between the two mice groups (Fig. 4C). Negative LV1 scores typically correlated with control mice, while positive LV1 scores correlated with LET mice. Following a leave-one-out cross validation (LOOCV) approach, several cytokines differentiated LET mice from control mice including IL-7, IL-13, IL-31, IL-1β and MIP-3α (cross validation class error average: 0.167) (Fig. 4D). Under an LPS-induction, LV1 continued to be a distinguishable variable where negative scores usually distinguished control mice and LET mice with positive scores (Fig. 5C). Unlike the previous LOOCV under T cell activation, only IL-12p40 from the LPS-induced cytokine data had a small, positive LV1 score (cross validation class error average: 0.278) (Fig. 5D). Altogether, the multivariate analysis of the cytokines released from splenocytes under different immune cell stimulations differentiated mice that underwent a letrozole treatment from those that

12

did not. We conclude that immune cells from LET mice are hyporesponsive to stimulation and generally have reduced pro-inflammatory cytokines.

DISCUSSION

In this study, single-cell RNA sequencing of pituitaries from letrozole-induced prepubertal mice revealed a change in neuroendocrine cell populations and immune cell infiltration that may influence the homeostasis of the HPG axis and PCOS pathophysiology. Additionally, a multivariate analysis of the cytokines secreted from splenocytes of the PCOS mouse model suggested hyporesponsive immune cells under different stimulated states, but generally, a reduction in systemic pro-inflammatory responses.

The clinical characteristics of PCOS are heterogenous, and animal models are relied on as a noninvasive method of studying the pathophysiology of PCOS. Abnormalities in the secretion of GnRH and LH in PCOS patients have suggested defects in the HPG axis as a contributor to ovarian dysfunction, including hypothalamic inflammation (16-18). In the present study, we confirmed an effect on the lactotropes of LET mice compared to the control mice in both cell number and a single-cell transcriptome level. Lactotropic cells were largely absent in LET mice and indicated a possible reduction in total prolactin secretion. While prolactin is mostly known for its regulatory role in breast development and lactation, the hormone has hundreds of additional functions which include those involved in metabolism (30-33). A decrease in serum prolactin levels has been reported in PCOS patients compared to those without the disorder in multiple studies (34,35). Low serum prolactin levels have also been associated with impaired glucose tolerance or insulin resistance, which can relate to overweight PCOS patients having an increased risk for type 2 diabetes mellitus (36,37). Indeed, these results remain consistent with the increased

weight and impaired glucose tolerance exhibited in the LET mice of this study. Although *Prl* was not a significant DEG in the lactotropes of LET mice, the gene was significantly down-regulated in the somatotrope population as well as the macrophage 1 cluster.

In contrast, DEGs significantly up-regulated in the lactotropes included two genes associated with gynecological cancers. While the risk of endometrial cancer is higher in PCOS individuals of any age, a study quantified the risks of other cancers for patients younger than 54 years and found ovarian cancer to be significantly increased (38,39). It is worth noting that obesity is a risk factor for several gynecological cancers; therefore, the up-regulation of both *Wfdc2* and *Gng3* may have been associated with the weight gain in LET mice rather than the etiology of PCOS (39).

Unexpectedly, two subpopulations of gonadotropes were identified with their own set of DEGs. The three DEGs in the second subpopulation are members of the kallikrein subfamily of serine proteases with a wide range of physiological functions (40). *Klk1b24*, *Klk1b21*, and *Klk1b27* generally degrade extracellular matrix proteins in interstitial areas surrounding cells and are reported to be responsive to androgens (41). Their up-regulation in the LET mice is consistent with the endogenous hyperandrogenemia induction and its effect on the gonadotropes. The mechanism behind the regulation of androgens on the serine proteases and its relevance to PCOS in the HPG axis require additional research, as only a subpopulation of the gonadotropes had significant DEGs encoding the proteases.

As stated before, prolactin was expressed in the immune cells of the pituitaries and listed as significantly down-regulated in LET mice. The role of prolactin in the immune system includes regulating both the innate and adaptive immune system via cytokine secretion stimulation and cytokine receptor expression (42,43). Multiple studies inhibiting

14

prolactin secretion, such as via hypophysectomy or a dopamine receptor agonist treatment on rats, observed a decrease in both the cellular and humoral immune response that only became restored when prolactin secretion was re-established (44,45). Prolactin is also involved in inflammatory responses; however, under certain conditions with other molecules, the hormone has mediated anti-inflammatory effects as well (46). Whether pro- or anti-inflammatory, prolactin is classified as a type-1 cytokine because of its ability to activate target cells (47). The hormone is extremely pleiotropic and versatile; therefore, it may contribute to maintaining HPG axis homeostasis with prolactin dysfunction possibly linking to PCOS development.

Compared to other immune cell clusters, one of the macrophage subtypes in the pituitaries of LET mice exhibited up-regulated genes associated cytokine secretion. *Irf7*, which codes for a transcription factor critical for the expression of type 1 interferons, was up-regulated in a macrophage subtype of LET mice. This aligned with a previous study detecting an increased level of IRF7 protein in the endometrium of PCOS patients (8). After an hyperandrogenemia induction, the signaling pathway of *Irf7* may be activated to increase the expression of proinflammatory cytokines in the LET mice. While an increased level of macrophages has been reported in PCOS ovarian tissue, the total number of macrophages were significantly lower in the pituitaries of LET mice (48). Excessive androgens inhibit macrophage viability and increase their apoptosis; therefore, the letrozole treatment may have affected the total population of macrophages in the neuroendocrine organ of the mice (49). However, the macrophages in the pituitaries of LET mice seemed to be involved in similar inflammatory responses detected in other immune microenvironments of PCOS patients, which could link to the progression of the disorder.

In contrast to the total macrophage population, a significantly larger presence of neutrophils was observed in the pituitaries of LET mice. Androgens influence the proliferation of neutrophils; however, the lymphocyte count must also be considered to determine the severity of systemic inflammation (50,51). The neutrophil-to-lymphocyte ratio, a proposed PCOS biomarker, is reported to be higher in PCOS patients compared to those without the disorder (51). The higher ratio is indicative of chronic inflammation, but at a local level, the neutrophils in the pituitaries of LET mice contained low-expressed genes involved in lipid metabolism and cellular homeostasis. Phospholipases in neutrophils are involved in lipid droplet formation and inflammatory mediator production for the cell's activation (52). Furthermore, androgens are capable of affecting neutrophils to suppres pro-inflammatory responses by decreasing extracellular signal-regulated kinase and leukotriene formation (53). Indeed, the inconsistent reports on the role of neutrophils in PCOS progression require further investigation, which may reveal additional relationships with metabolic and hormonal parameters.

The spleen is a reflective organ of systemic inflammation because of its function in replenishing immune cells to various tissues. Under different stimulations, the spleens from LET mice may be investigated to gain a reflection of the systemic immune response in PCOS patients. Whether the splenocytes from the LET mice underwent a T cell-specific or an LPS induced activation, a general reduction in pro-inflammatory cytokines was observed compared to the control mice. This is contrary to studies analyzing either the plasma or peripheral blood of PCOS patients in which cytokines, such as IL-6 and MIP1A, were elevated (54,55). Additional research on the immune cell populations in the spleens must be executed to confirm whether a reduction in pro-inflammatory cytokine levels

16

aligns with a decrease in the immune cell population. Despite the discrepancy in cytokine data from mouse spleen to that in serum of PCOS patients, PLS-DA performed from their overall cytokine profiles under different stimulations managed to separate the mice based on whether they were treated with letrozole or a placebo.

In conclusion, the pituitaries of letrozole-induced PCOS mice experienced a reduction in lactotropes and disease-specific immune responses within their microenvironment involving prolactin secretion. Despite cytokine profiles from stimulated splenocytes generally representing reduced pro-inflammatory responses, they were distinct enough to produce a predictive model for PCOS. The disparity in inflammatory states, whether at a local level or a systemic level, requires additional research to clarify underlying mechanisms possibly responsible for the heterogeneity in PCOS pathophysiology. The results of the present study provide an increased understanding of the extent to which an animal model is representative of the immune system in PCOS.
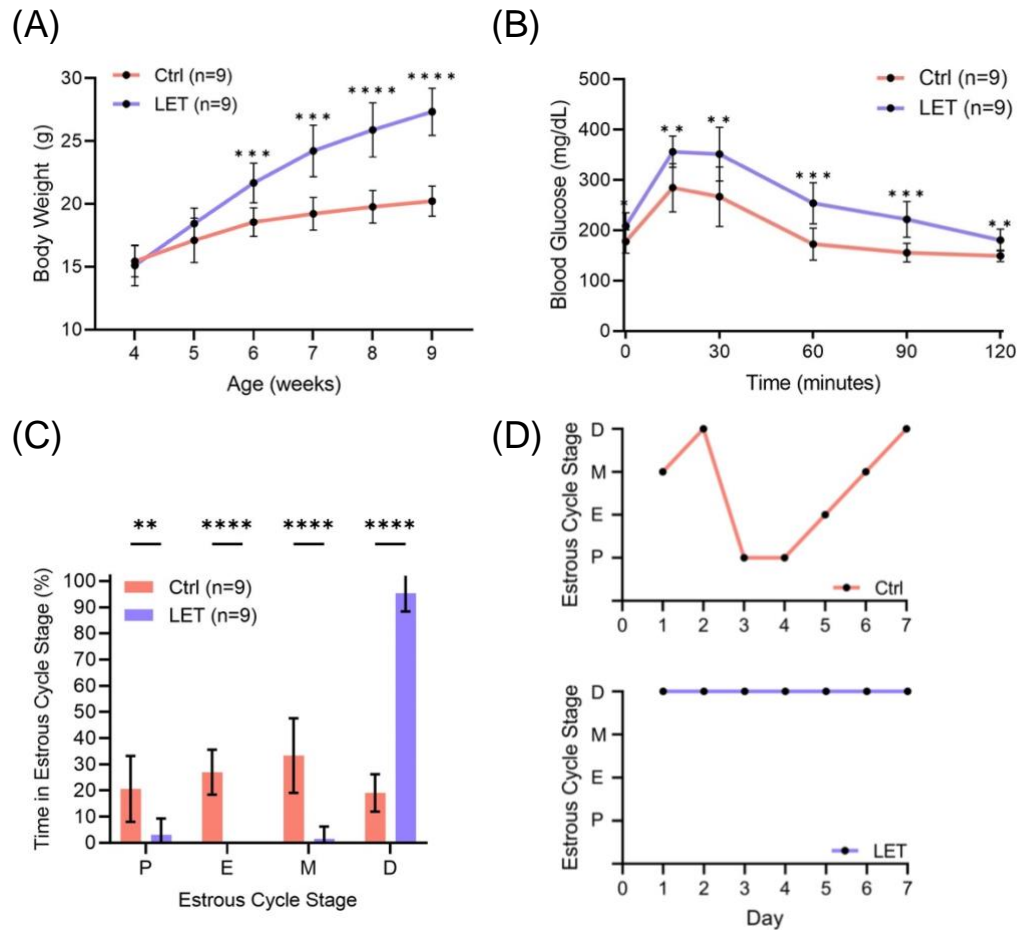
Figure 1. 5-week letrozole treatment on prepubertal female mice developed both reproductive and metabolic phenotypes of PCOS. Letrozole-treated mice (LET; n=9) experienced increased body weight (A), impaired glucose tolerance tests (B), and acyclicity (C) compared to placebo-treated mice (Ctrl; n=9). A representative estrous cycle of a Ctrl mouse and a LET mouse is given (D). * p≤0.05, ** p≤0.01, *** p≤0.001, **** p≤0.0001, Student's t-test. Error bars are mean ± SD. P, proestrous. E, estrous. M, metestrus. D, diestrus.
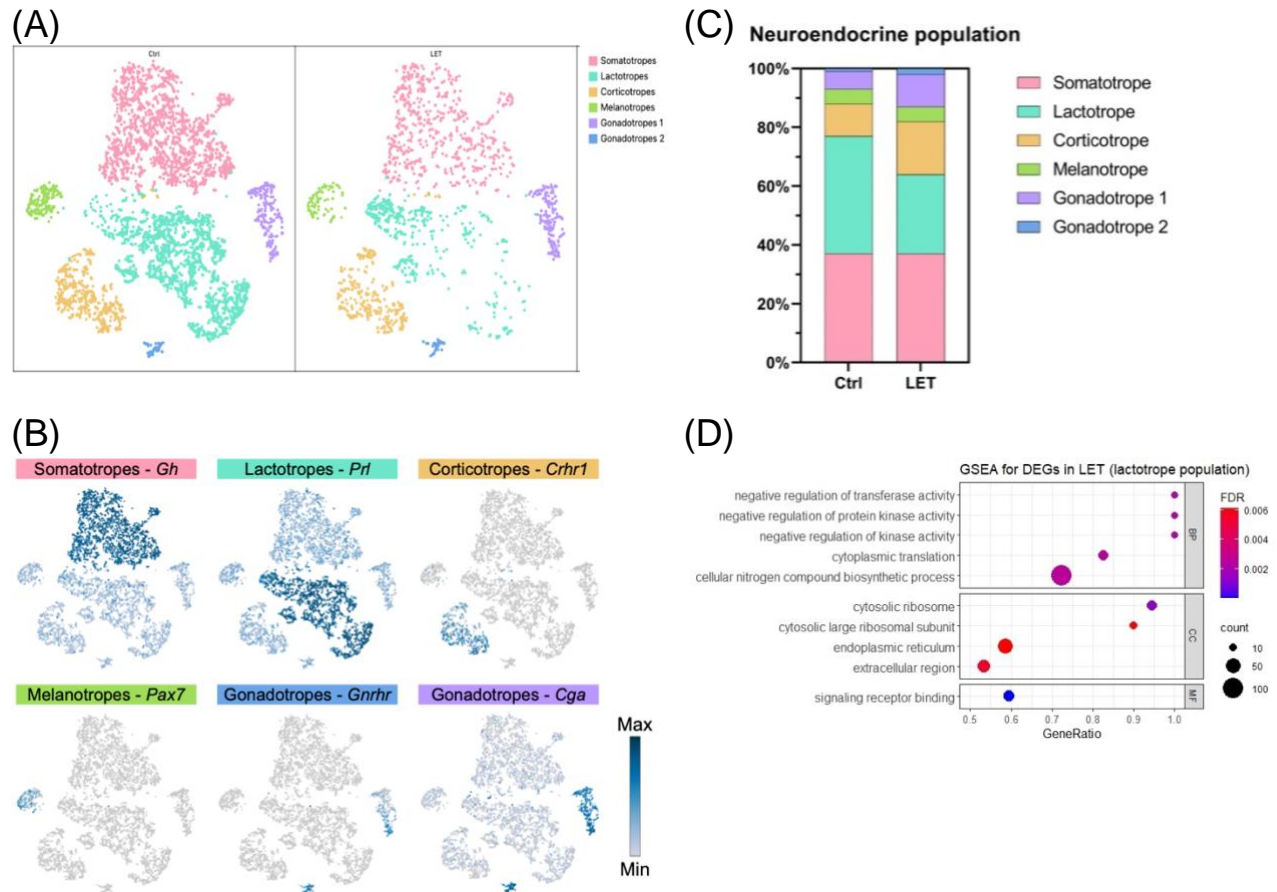
Figure 2. scRNA-seq analysis of the pituitary endocrine cells of placebo and letrozole-treated prepubertal female mice. (A) tSNE plots visualizing 4,536 pituitary endocrine cells from Ctrl mice (n=5) and 1,781 pituitary endocrine cells from LET mice (n=5) in manually assigned subtypes. (B) The expression of *Gh*, *Prl*, *Crhr1*, *Pax7*, *Gnrhr*, and *Cga* to mark the clusters into somatotropes, lactotropes, corticotropes, melanotropes, and gonadotropes respectively in the aggregated data of both Ctrl and LET mice. The minimum log2 expression (min) is 0 counts and the maximum log2 expression (Max) varied from 3 to 15 counts depending on the gene. (C) The distribution of cell types in the pituitary neuroendocrine population of both mice groups. (D) GSEA based on the significant DEGs (|Log2FC|≥1.5; p≤0.05) in the lactotropes of LET mice compared to Ctrl mice. BP, biological process. CC, cellular component. MF, molecular function. FDR, false discovery rate.
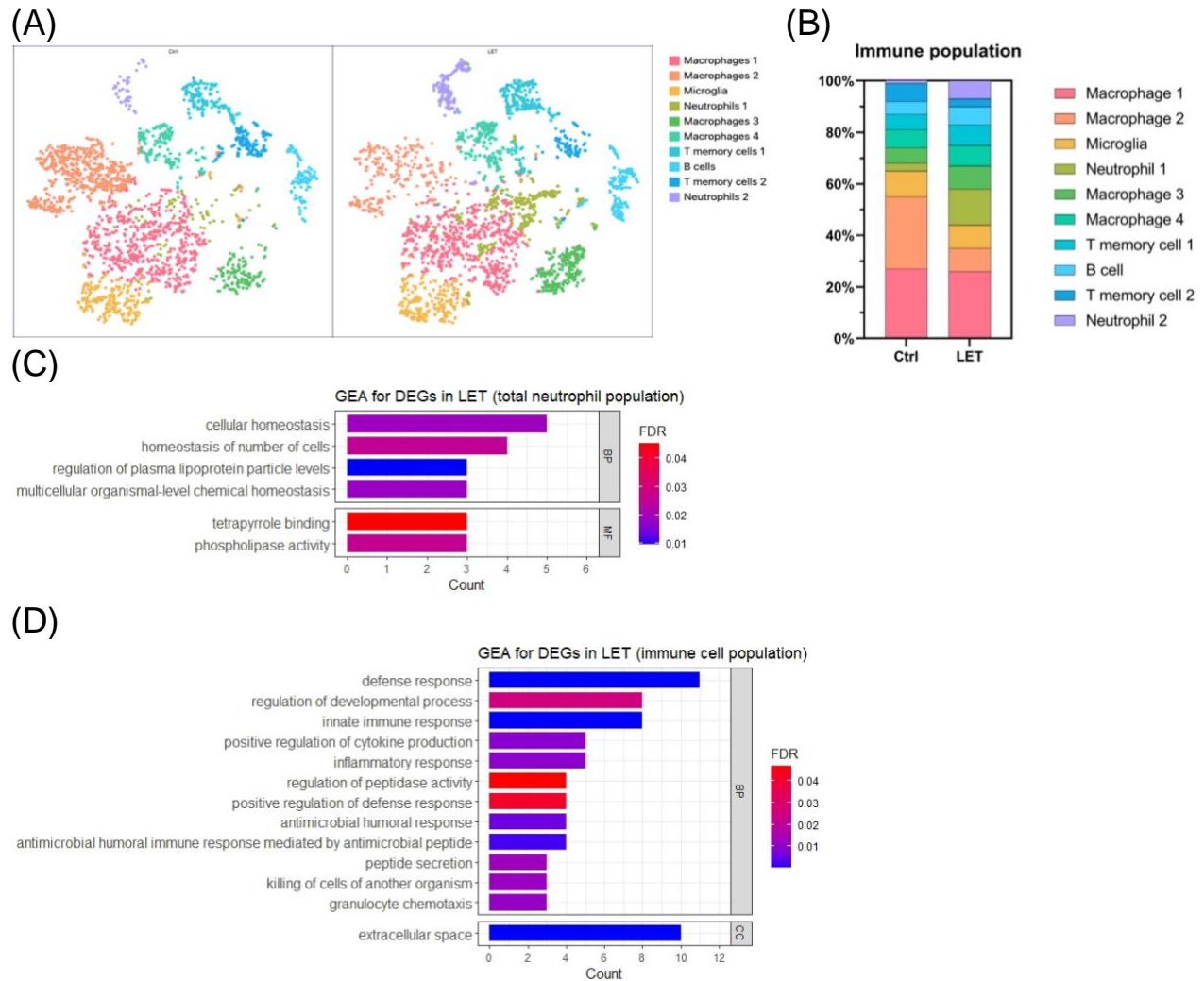
Figure 3. scRNA-seq analysis of the immune cell population in the pituitary of placebo and letrozole-treated prepubertal female mice. (A) tSNE plots visualizing 2,430 immune cells from Ctrl mice pituitaries (n=5) and 2,816 immune cells from LET mice pituitaries (n=5) in manually assigned subtypes. (B) The distribution of cell types in the immune cell population of both mice groups. (C) GEA based on the down-regulated DEGs (|Log2FC|≥1.5; p≤0.05) in the total neutrophil population of LET mice. (D) GEA based on the significant DEGs (|Log2FC|≥1.5; p≤0.05) in the total immune cell population of LET mice. BP, biological process. CC, cellular component. MF, molecular function. FDR, false discovery rate.
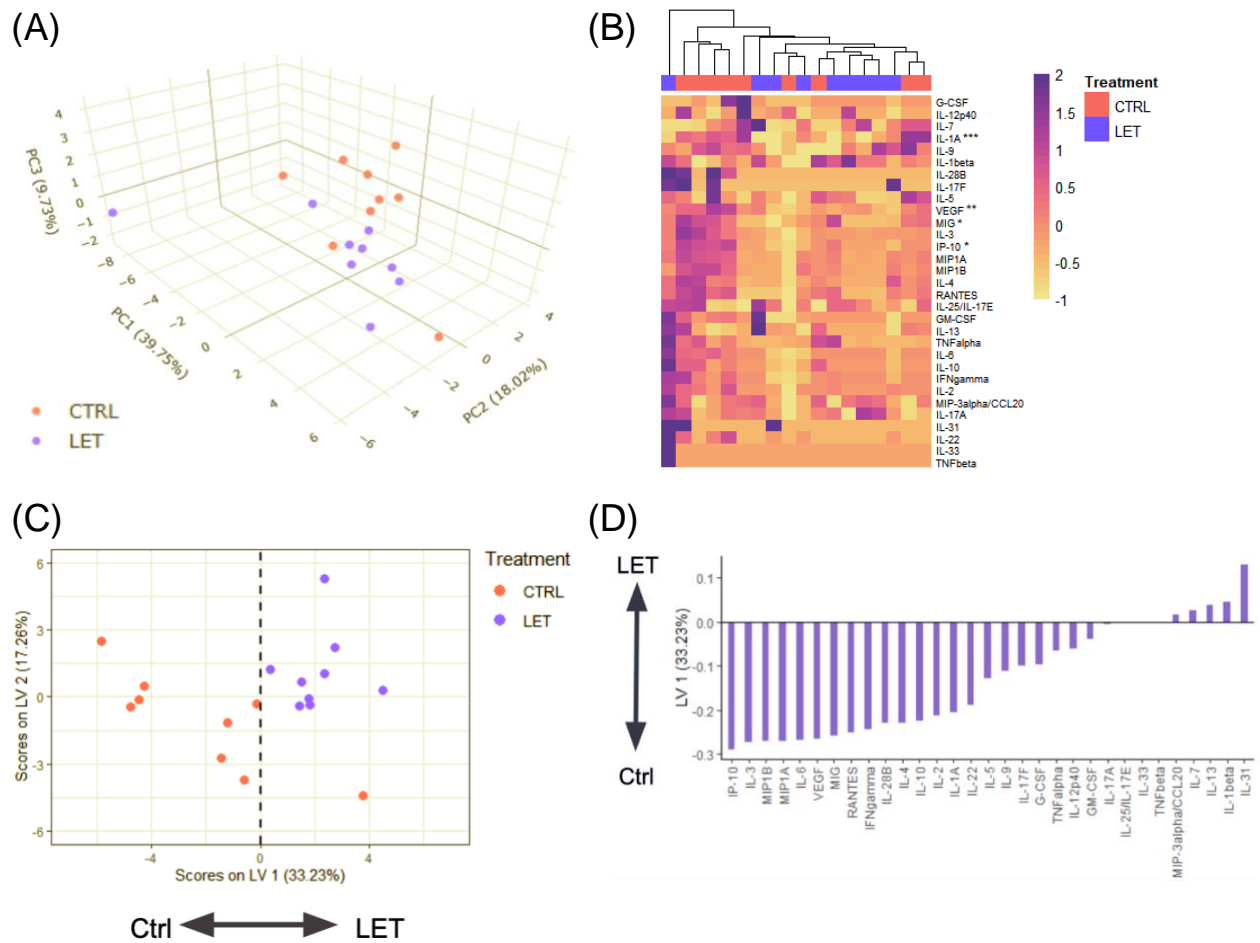
Figure 4. Multiplexed immunoassay cytokine analysis on the conditioned media of CD3/28-activated splenocytes from control and LET mice. (A) PCA plot of the cytokine profiles. (B) Heat map of z-scored and batch corrected cytokine quantification data grouped via hierarchical clustering. (C) PLS-DA separated the Ctrl mice (n=9) to the left and the LET mice (n=9) to the right along LV1. (D) The cytokine profiles correlated with either the Ctrl mice (negative) or the LET mice (positive) on the new LV1 axis. * p≤0.05, ** p≤0.01, *** p≤0.001, Student's t-test.
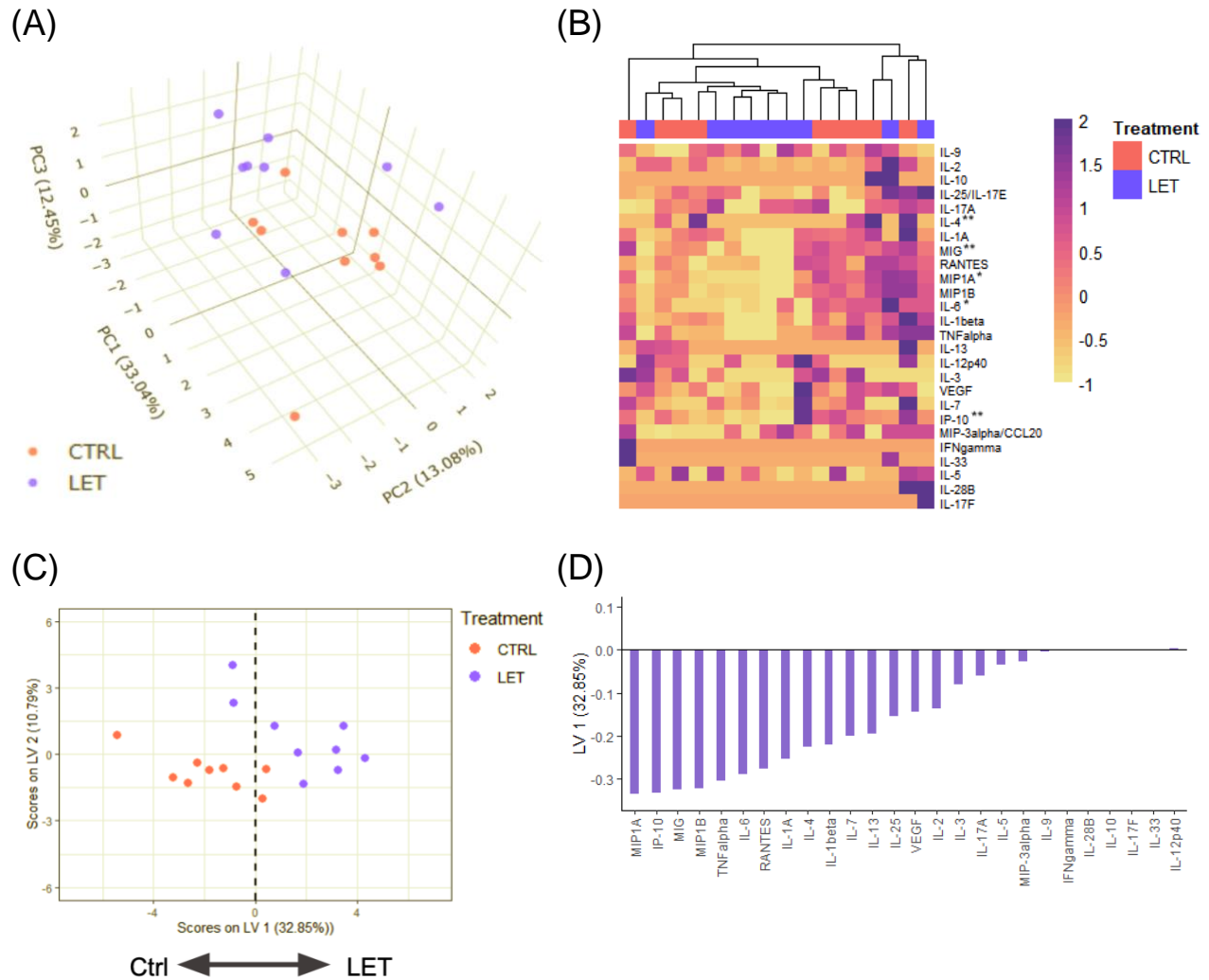
Figure 5. Multiplexed immunoassay cytokine analysis on the conditioned media of LPS-activated splenocytes from control and LET mice. (A) PCA plot of the cytokine profiles. (B) Heat map of z-scored and batch corrected cytokine quantification data grouped via hierarchical clustering. (C) PLS-DA separated the Ctrl mice (n=9) to the left and the LET mice (n=9) to the right along LV1. (D) The new LV1 axis of the cytokine profiles did not separate between the Ctrl mice and the LET mice. * p≤0.05, ** p≤0.01, Student's t-test.

Table 1. Differentially expressed genes (|Log2FC|≥1.5) related to the letrozole-induced PCOS mouse model in neuroendocrine cell sub-populations from the pituitary.

Somatotropes		
Gene	Log2 FC	P-value
Prl	-3.24	1.34×10^{-4}
Lactotropes		
Gene	Log2 FC	P-value
Crhbp	-3.12	8.36×10^{-10}
Nrxn3	-1.85	1.48×10^{-4}
Wfdc2	4.81	3.47×10^{-30}
Nnat	2.96	6.36×10^{-24}
Thy1	2.77	2.14×10^{-17}
Ly6h	2.70	7.14×10^{-20}
Uchl1	2.56	2.27×10^{-17}
Gng3	2.44	4.59×10^{-16}
CAAA01147332.1	2.03	1.45×10^{-10}
Ptn	1.96	8.39×10^{-10}
Lrpap1	1.95	5.95×10^{-10}
Pcp4	1.92	8.99×10^{-8}
Prdx4	1.83	9.28×10^{-9}
Ssr4	1.79	6.57×10^{-9}
Stmn1	1.77	1.39×10^{-7}
Nenf	1.68	1.45×10^{-7}
Ly6e	1.59	3.17×10^{-6}
Spint2	1.53	2.82×10^{-6}
Tmem59l	1.53	5.04×10^{-6}
Gm1673	1.50	1.33×10^{-5}
Corticotropes		
Gene	Log2 FC	P-value
Srxn1	-1.90	2.50×10^{-3}
Gonadotropes 1		
Gene	Log2 FC	P-value
Lhb	-2.06	1.07×10^{-3}
Gonadotropes 2		
Gene	Log2 FC	P-value
Klk1b24	5.09	2.15×10^{-4}
Klk1b21	4.55	2.92×10^{-3}
Klk1b27	3.71	1.93×10^{-2}

Table 2. Differentially expressed genes (|Log2FC|≥1.5) related to the letrozole-induced PCOS mouse model in immune cell sub-populations from the pituitary.

Macrophages 1		
Gene	Log2 FC	P-value
Prl	-3.42	7.60×10^{-5}
Macrophages 3		
Gene	Log2 FC	P-value
Fos	-1.80	2.02×10^{-2}
Ccl5	2.58	2.02×10^{-2}
Macrophages 4		
Gene	Log2 FC	P-value
Mt1	-1.84	1.60×10^{-2}
Fscn1	4.46	3.16×10^{-3}
Ccr7	3.06	1.60×10^{-2}
Ccl5	2.90	1.60×10^{-2}
Isg15	2.32	2.22×10^{-2}
F13a1	2.03	1.60×10^{-2}
Ass1	1.86	1.60×10^{-2}
Irf7	1.74	3.86×10^{-2}
Neutrophils 1		
Gene	Log2 FC	P-value
Slc40a1	-3.73	1.94×10^{-3}
Clec4n	-3.50	2.80×10^{-2}
Igf1	-2.99	1.05×10^{-4}
Lpl	-2.75	1.94×10^{-3}
Hmox1	-2.64	1.38×10^{-3}
Slc48a1	-2.16	2.56×10^{-2}
Pla2g7	-1.96	2.80×10^{-2}
Creg1	-1.85	2.80×10^{-2}
Neutrophils 2		
Gene	Log2 FC	P-value
Lmo4	-2.00	4.08×10^{-3}
Malat1	-1.67	2.72×10^{-2}
T memory cells 1		
Gene	Log2 FC	P-value
Isg15	2.89	1.88×10^{-2}

REFERENCES

1. Deswal, R., Narwal, V., Dang, A. and Pundir, C.S. (2020). The Prevalence of Polycystic Ovary Syndrome: A Brief Systematic Review. *Journal of Human Reproductive Sciences*, 13(4), pp.261–271.
2. Ben-Shlomo, I. and Younis, J.S. (2014). Basic research in PCOS: are we reaching new frontiers? *Reproductive BioMedicine Online*, 28(6), pp.669–683.
3. Stener-Victorin, E., Padmanabhan, V., Walters, K.A., Campbell, R.E., Benrick, A., Giacobini, P., Dumesic, D.A. and Abbott, D.H. (2020). Animal Models to Understand the Etiology and Pathophysiology of Polycystic Ovary Syndrome. *Endocrine Reviews*, 41(4), pp.538–576.
4. Kauffman, A.S., Thackray, V.G., Ryan, G.E., Tolson, K.P., Glidewell-Kenney, C.A., Semaan, S.J., Poling, M.C., Iwata, N., Breen, K.M., Duleba, A.J., Stener-Victorin, E., Shimasaki, S., Webster, N.J. and Mellon, P.L. (2015). A Novel Letrozole Model Recapitulates Both the Reproductive and Metabolic Phenotypes of Polycystic Ovary Syndrome in Female Mice1. *Biology of Reproduction*, 93(3).
5. Rudnicka, E., Suchta, K., Grymowicz, M., Calik-Ksepka, A., Smolarczyk, K., Duszewska, A.M., Smolarczyk, R. and Meczekalski, B. (2021). Chronic Low Grade Inflammation in Pathogenesis of PCOS. *International Journal of Molecular Sciences*, 22(7).
6. Zhai, Y. and Pang, Y. (2022). Systemic and ovarian inflammation in women with polycystic ovary syndrome. *Journal of Reproductive Immunology*, 151, p.103628.
7. Rostamtabar, M., Esmaeilzadeh, S., Tourani, M., Rahmani, A., Baee, M., Shirafkan, F., Saleki, K., Mirzababayi, S.S., Ebrahimpour, S. and Nouri, H.R. (2020). Pathophysiological roles of chronic low-grade inflammation mediators in polycystic ovary syndrome. *Journal of Cellular Physiology*, 236(2), pp.824–838.
8. Hu, M., Zhang, Y., Li, X., Cui, P., Sferruzzi-Perri, A.N., Mats Brännström, Shao, L.R. and Billig, H. (2021). TLR4-Associated IRF-7 and NFκB Signaling Act as a Molecular Link Between Androgen and Metformin Activities and Cytokine Synthesis in the PCOS Endometrium. *The Journal of Clinical Endocrinology & Metabolism*, 106(4), pp.e1022–e1040.
9. Escobar-Morreale, H.F., Botella-Carretero, J.I., Villuendas, G., Sancho, J. and San Millán, J.L. (2004). Serum Interleukin-18 Concentrations Are Increased in the Polycystic Ovary Syndrome: Relationship to Insulin Resistance and to Obesity. *The Journal of Clinical Endocrinology & Metabolism*, 89(2), pp.806–811.
10. Zhang, H., Wang, X., Xu, J., Zhu, Y., Chen, X. and Hu, Y. (2020). IL-18 and IL-18 binding protein concentration in ovarian follicular fluid of women with unexplained infertility to PCOS during in vitro fertilization. *Journal of Reproductive Immunology*, 138, p.103083.
11. Dorte Glintborg, Andersen, M., Bjørn Richelsen and Bruun, J.M. (2009). Plasma monocyte chemoattractant protein-1 (MCP-1) and macrophage inflammatory protein-1α are increased in patients with polycystic ovary syndrome (PCOS) and associated with adiposity, but unaffected by pioglitazone treatment. *Clinical Endocrinology*, 71(5), pp.652–658.

12. González, F., Rote, N.S., Minium, J., Weaver, A.L. and Kirwan, J.P. (2010). Elevated circulating levels of macrophage migration inhibitory factor in polycystic ovary syndrome. *Cytokine*, 51(3), pp.240–244.
13. Qin, L., Xu, W., Li, X., Meng, W., Hu, L., Luo, Z., Wang, Y., Luo, S. and Li, S. (2016). Differential Expression Profile of Immunological Cytokines in Local Ovary in Patients with Polycystic Ovarian Syndrome: analysis by Flow Cytometry. *European Journal of Obstetrics & Gynecology and Reproductive Biology*, 197, pp.136–141.
14. Charles, Oliveira, T.Y., Miranda-Alves, L., Alessandra Simão Padilha, Krause, M., Maria João Carneiro, Salgado, B.S. and Jones Bernardes Graceli (2021). Subacute cadmium exposure disrupts the hypothalamic-pituitary-gonadal axis, leading to polycystic ovarian syndrome and premature ovarian failure features in female rats. *Environmental Pollution*, 269, pp.116154–116154.
15. Wang, F., Zhang, Z.-H., Xiao, K.-Z. and Wang, Z.-C. (2017). Roles of Hypothalamic-Pituitary-Adrenal Axis and Hypothalamus-Pituitary-Ovary Axis in the Abnormal Endocrine Functions in Patients with Polycystic Ovary Syndrome. *Zhongguo Yi Xue Ke Xue Yuan Xue Bao. Acta Academiae Medicinae Sinicae*, 39(5), pp.699–704.
16. Szeliga, A., Rudnicka, E., Maciejewska-Jeske, M., Kucharski, M., Kostrzak, A., Hajbos, M., Niwczyk, O., Smolarczyk, R. and Meczekalski, B. (2022). Neuroendocrine Determinants of Polycystic Ovary Syndrome. *International Journal of Environmental Research and Public Health*, 19(5), p.3089.
17. Barlampa, D., Bompoula, M.S., Bargiota, A., Kalantaridou, S., Mastorakos, G. and Valsamakis, G. (2021). Hypothalamic Inflammation as a Potential Pathophysiologic Basis for the Heterogeneity of Clinical, Hormonal, and Metabolic Presentation in PCOS. *Nutrients*, 13(2), p.520.
18. Lian, Y., Zhao, F. and Wang, W. (2016). Central leptin resistance and hypothalamic inflammation are involved in letrozole-induced polycystic ovary syndrome rats. *Nutrients*, 476(4), pp.306–312.
19. McCartney, C.R. and Campbell, R.E. (2020). Abnormal GnRH pulsatility in polycystic ovary syndrome: Recent insights. *Current Opinion in Endocrine and Metabolic Research*, 12, pp.78–84.
20. Coutinho, E. and Kauffman, A. (2019). The Role of the Brain in the Pathogenesis and Physiology of Polycystic Ovary Syndrome (PCOS). *Medical Sciences*, 7(8), p.84.
21. Kenealy, B.P., Kapoor, A., Guerriero, K.A., Keen, K.L., Garcia, J.P., Kurian, J.R., Ziegler, T.E. and Terasawa, E. (2013). Neuroestradiol in the Hypothalamus Contributes to the Regulation of Gonadotropin Releasing Hormone Release. *Journal of Neuroscience*, 33(49), pp.19051–19059.
22. Coyle, C.A., Prescott, M., Handelsman, D.J., Walters, K.A. and Campbell, R. (2022). Chronic androgen excess in female mice does not impact luteinizing hormone pulse frequency or putative GABAergic inputs to GnRH neurons. *Journal of Neuroendocrinology,* 34(4).
23. Franzén, O., Gan, L.-M. and Björkegren, J.L.M. (2019). PanglaoDB: a web server for exploration of mouse and human single-cell RNA sequencing data. *Database*, 2019.
24. Ashburner, M., Ball, C.A., Blake, J.A., Botstein, D., Butler, H., Cherry, J.M., Davis, A.P., Dolinski, K., Dwight, S.S., Eppig, J.T., Harris, M.A., Hill, D.P., Issel-Tarver, L., Kasarskis, A., Lewis, S., Matese, J.C., Richardson, J.E., Ringwald, M., Rubin, G.M. and Sherlock, G.

(2000). Gene Ontology: tool for the unification of biology. *Nature Genetics*, 25(1), pp.25–29.

25. Aleksander, S., Balhoff, J.P., Carbon, S., J. Michael Cherry, Drabkin, H.J., Ebert, D., Feuermann, M., Gaudet, P., Harris, N.L., Hill, D.P., Lee, R., Mi, H., Sierra, Mungall, C.J., Anushya Muruganujan, Tremayne Mushayahama, Sternberg, P.W., Thomas, P., Van, K.M. and Ramsey, J. (2023). The Gene Ontology knowledgebase in 2023. *Genetics*, 224(1).

26. Thomas, P.D., Ebert, D., Muruganujan, A., Mushayahama, T., Albou, L. and Mi, H. (2021). PANTHER : Making genome-scale phylogenetics accessible to all. *Protein Science*, 31(1), pp.8–22.

27. Mukherjee, S., Sundfeldt, K., Carl A.K. Borrebaeck and Jakobsson, M.E. (2021). Comprehending the Proteomic Landscape of Ovarian Cancer: A Road to the Discovery of Disease Biomarkers. *Proteomes*, 9(2), pp.25–25.

28. Yin, X., Wang, P., Yang, T., Li, G., Teng, X., Huang, W. and Yu, H. (2021). Identification of key modules and genes associated with breast cancer prognosis using WGCNA and ceRNA network analysis. *Aging*, 13(2), pp.2519–2538.

29. Goffin, V., Binart, N., Touraine, P. and Kelly, P.A. (2002). Prolactin: The New Biology of an Old Hormone. *Annual Review of Physiology*, 64(1), pp.47–67.

30. Patil, M., Belugin, S., Mecklenburg, J., Wangzhou, A., Paige, C., Barba-Escobedo, P.A., Boyd, J.T., Goffin, V., Grattan, D., Boehm, U., Dussor, G., Price, T.J. and Akopian, A.N. (2019). Prolactin Regulates Pain Responses via a Female-Selective Nociceptor-Specific Mechanism. *iScience*, 20, pp.449–465.

31. Arnold, E., Thébault, S., Aroña, R.M., Martínez de la Escalera, G. and Clapp, C. (2020). Prolactin mitigates deficiencies of retinal function associated with aging. *Neurobiology of Aging*, 85, pp.38–48.

32. Jiao, P., Yuan, Y., Zhang, M.-M., Sun, Y., Wei, C., Xie, X., Zhang, Y., Wang, S., Chen, Z. and Wang, X. (2020). PRL/microRNA-183/IRS1 Pathway Regulates Milk Fat Metabolism in Cow Mammary Epithelial Cells. *Genes*, 11(2), pp.196–196.

33. Rahbar, A., AlKharusi, A., Costa, H., Pantalone, M.R., Kostopoulou, O.N., Cui, H.L., Carlsson, J., Rådestad, A.F., Söderberg-Naucler, C. and Norstedt, G. (2020). Human Cytomegalovirus Infection Induces High Expression of Prolactin and Prolactin Receptors in Ovarian Cancer. *Biology*, 9(3), p.44.

34. Glintborg, D., Altinok, M., Mumm, H., Buch, K., Ravn, P. and Andersen, M. (2014). Prolactin is associated with metabolic risk and cortisol in 1007 women with polycystic ovary syndrome. *Human Reproduction*, 29(8), pp.1773–1779.

35. Yang, H., Di, J., Pan, J., Yu, R., Teng, Y., Cai, Z. and Deng, X. (2020). The Association Between Prolactin and Metabolic Parameters in PCOS Women: A Retrospective Analysis. *Frontiers in Endocrinology*, 11.

36. Wang, T., Lu, J., Xu, Y., Li, M., Sun, J., Zhang, J., Xu, B., Xu, M., Chen, Y., Bi, Y., Wang, W. and Ning, G. (2013). Circulating Prolactin Associates With Diabetes and Impaired Glucose Regulation: A population-based study. *Diabetes Care*, 36(7), pp.1974–1980.

37. Legro, R.S., Kunselman, A.R., Dodson, W.C. and Dunaif, A. (1999). Prevalence and Predictors of Risk for Type 2 Diabetes Mellitus and Impaired Glucose Tolerance in Polycystic Ovary Syndrome: A Prospective, Controlled Study in 254 Affected Women1. *The Journal of Clinical Endocrinology & Metabolism*, 84(1), pp.165–169.

38. Teede, H.J., Misso, M.L., Costello, M.F., Dokras, A., Laven, J., Moran, L., Piltonen, T. and Norman, R.J. (2018). Erratum. Recommendations from the international evidence-based guideline for the assessment and management of polycystic ovary syndrome. *Human Reproduction*, 34(2), pp.388–388.

39. Barry, J.A., Azizia, M.M. and Hardiman, P.J. (2014). Risk of endometrial, ovarian and breast cancer in women with polycystic ovary syndrome: a systematic review and meta-analysis. *Human Reproduction Update*, 20(5), pp.748–758.

40. Clements, J.A., Willemsen, N.M., Myers, S.P. and Dong, Y. (2004). The Tissue Kallikrein Family of Serine Proteases: Functional Roles in Human Disease and Potential as Clinical Biomarkers. *Critical Reviews in Clinical Laboratory Sciences*, 41(3), pp.265–312.

41. Lawrence, M.G., Lai, J. and Clements, J.A. (2010). Kallikreins on Steroids: Structure, Function, and Hormonal Regulation of Prostate-Specific Antigen and the Extended Kallikrein Locus. *Endocrine Reviews*, 31(4), pp.407–446.

42. Moreno, J., Varas, A., Vicente, A. and Zapata, A.G. (1998). Role of Prolactin in the Recovered T-Cell Development of Early Partially Decapitated Chicken Embryo. *Developmental Immunology*, 5(3), pp.183–195.

43. Peeva, E. and Zouali, M. (2005). Spotlight on the role of hormonal factors in the emergence of autoreactive B-lymphocytes. *Immunology Letters*, 101(2), pp.123–143.

44. Nagy, E. and Istvan Berczi (1978). IMMUNODEFICIENCY IN HYPOPHYSECTOMIZED RATS. *Acta Endocrinologica*, 89(3), pp.530–537.

45. Nagy, E., Berczi, I., Wren, G.E., Asa, S.L. and Kovacs, K. (1983). Immunomodulation by bromocriptine. *Immunopharmacology*, 6(3), pp.231–243.

46. Ramos-Martinez, E., Ramos-Martínez, I., Molina-Salinas, G., Zepeda-Ruiz, W.A. and Cerbon, M. (2021). The role of prolactin in central nervous system inflammation. *Reviews in the Neurosciences*, 32(3), pp.323-340.

47. Huising, M.O., Kruiswijk, C.P. and Flik, G. (2006). Phylogeny and evolution of class-I helical cytokines. *Journal of Endocrinology*, 189(1), pp.1–25.

48. Xiong, Y., Liang, X., Yang, X., Li, Y. and Li Na Wei (2011). Low-grade chronic inflammation in the peripheral blood and ovaries of women with polycystic ovarian syndrome. *European Journal of Obstetrics & Gynecology and Reproductive Biology*, 159(1), pp.148–150.

49. Li, X., Li, L., Ouyang Dimei, Zhu, Y. and Yuan, T. (2021). The abnormal expression of kisspeptin regulates pro-inflammatory cytokines, cell viability and apoptosis of macrophages in hyperandrogenism induced by testosterone. *Gynecological Endocrinology*, 37(1), pp.72–77.

50. Segner, H., Verburg-van Kemenade, B.M.L. and Chadzinska, M. (2017). The immunomodulatory role of the hypothalamus-pituitary-gonad axis: Proximate mechanism for reproduction-immune trade offs? *Developmental & Comparative Immunology*, 66, pp.43–60.

51. Li, L., Yu, J., and Zhou, Z. (2022). Association between neutrophil-to-lymphocyte ratio and polycystic ovary syndrome: a PRISMA-complaint systematic review and meta-analysis. *Medicine (Baltimore)*, 101(38), p.e30579.

52. Jiang, J., Tu, H. and Li, P. (2022). Lipid metabolism and neutrophil function. *Cellular Immunology*, 377, p.104546.

53. Wang, J., Yin, T., and Liu, S. (2023). Dysregulation of immune response in PCOS organ system. *Frontiers in immunology*, 14.

54. Glintborg, D., Andersen, M., Richelsen, B., and Bruun, J.M. (2009). Plasma monocyte chemoattractant protein-1 (MCP-1) and macrophage inflammatory protein-1α are increased in patients with polycystic ovary syndrome (PCOS) and associated with adiposity, but unaffected by pioglitazone treatment. *Clinical Endocrinology*, 71(5), pp.652–658.
55. Borthakur, A., D Prabhu, Y. and Valsala Gopalakrishnan, A. (2020). Role of IL-6 signaling in Polycystic Ovarian Syndrome associated inflammation. *Journal of Reproductive Immunology*, 141, p.103155.